ACTA GEOPHYSICA POLONICA
Vol.XXXIX, no.2 1991

# ANALYSIS OF THE MAGNETO-TELLURIC RECORDINGS FROM THE FRIULI SEISMIC ZONE, NE ITALY

Tomasz ERNST, Janusz MARIANIUK, Cezary P. ROZŁUSKI,
Jerzy JANKOWSKI, Antoni PAŁKA, Roman TEISSEYRE
Institute of Geophysics, Polish Academy of Sciences
01-452 Warsaw, ul. Księcia Janusza 64

Carla BRAITENBERG, Maria ZADRO
Institute of Geodesy and Geophysics, University of Triest
Via Universita 7, Triest, Italy

A b s t r a c t

In the period 1987/88 the magneto-telluric measurements were carried out around Friuli, North-East Italy, seismic area. The purpose was to find a possible correlation between the magneto-telluric signals and seismic activity.

Two stations have been equipped with digital magnetic and telluric recorders, and a third station with telluric and resistivity recorders. Magnetic recordings give a possibility to subtract from the telluric field the natural variations; also, some artificial disturbances can be eliminated by suitable computer programs for transfer function.

New original methods have been proposed in searching for the tectonic related signals. Before some shocks in the Friuli region in September 1987 and February 1988 we have found some unusual telluric activity.

## 1. Introduction

Electric and magnetic precursory phenomena have been reported by many authors; here we confine ourselves to remind only a few selected papers on telluric and resistivity variations. Sobolev (1975) has observed bay-type telluric anomalies preceding some earthquakes, more recently Varotsos and Alexopoulos (1984) have reported appearances of short-type seismic electric signals (SES), precursory to seismic events in Greece. Reports on resistivity variations (e.g., Yamazaki, 1975; Rikitake, 1976) show a somewhat higher consistency, but there still big differences in the observed range of resistivity changes before seismic events. Usually they are very small, but for some very local tremors in mines (observations at a few hundred meters) Stopiński and Teisseyre (1982) reported changes exceeding the order of the primary resistivity value.

The telluric field in its main part is related to magnetic variations through electromagnetic induction in the crust and mantle; however, there appear also many other contributions to this field, e.g., due to industrial disturbances, high tension lines and electric trains. To find a tectonic related component and to discriminate it by suitable numerical procedures from other sources remains a very difficult task. The fully successful results can be obtained only when recording is done in places characterized by a relatively low artificial noise level.

Nevertheless, it is reasonable to believe that the electric field related to mechanical fracturing processes may serve as a very sensitive precursor of earthquakes. Electric resistivity is another important property which can be studied in a seismic area; a possible crack induced resistivity anisotropy shall be here taken into account.

The Friuli area was selected as a test area, as it is a rather restricted seismic region, and other local networks are already in operation there.

The geological and geodynamical characteristics of Friuli are peculiar as two different mountain ranges merge there: the Southern Alps and the Dinarides. The main difference between them is the orientation of their main structural traces; the Alps displaying an E-W, the Dinarides a NW-SE orientation.

From 1976, the year of disastrous Friuli earthquake, a tiltmeter and strainmeter network was installed in the region by the Institute of Geodesy and Geophysics of the University of Trieste and has been continuously operative up to date. Furthermore since 1977 the seismicity of the region has been monitored by a teleseismic network (Osservatorio Geofisico Sperimentale, Trieste).

The electromagnetic campaign, including magneto-telluric and resistivity recordings, took place from July 1987 to June 1988, as a joint program of the Institute of Geodesy and Geophysics of the University of Trieste and of the Institute of Geophysics, Polish Academy of Sciences.

Three localizations have been selected for magnetic, telluric and resistivity recording sites. The magneto-telluric and resistivity instruments have been assembled and tested in the Belsk Observatory, Poland, before their installation in Friuli. As said, three stations were put in operation in Friuli: Forni di Sotto "FDS" (three geomagnetic field components, two electrical horizontal components); Castelmonte (Iainich) "IAI" with the same equipment, and Villanova "VIL" with resistivity and telluric recording instruments.

On Fig. 1, there are indicated the locations of the magneto-telluric and resistivity stations used in our campaign.

From the beginning we have been aware of rather high industrial disturbances (also railways) in the NE Italian region, but only after the first results we found that a very low resistivity zone extends down to a depth of 10-15 km. We can mention here that the hypocentres in this area are not deeper than 15 km. This means that the possible telluric signals might be greatly dissipated. In spite of rather unfavorable conditions, we found some results interesting enough to be reported here.

To find and interpret some unusual telluric signals, probably related to tectonic activity we have developed special research program and methods of data treatment in the following directions:

- find the apparent resistivity curves using the natural geomagnetic variations and, assuming horizontal layering, determine the resistivity structure at depth;

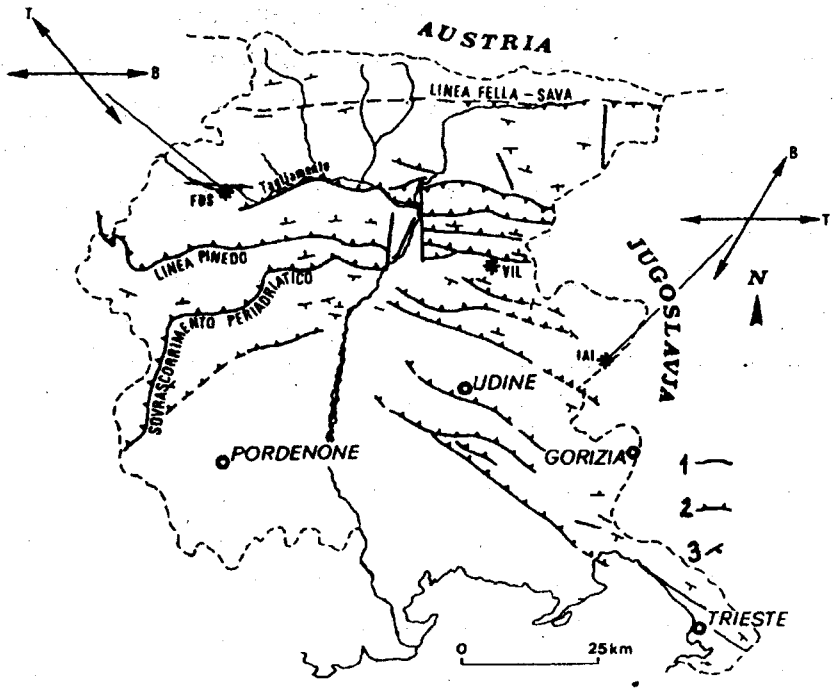


Fig. 1. Positions of the magnetotelluric stations in the Friuli area. The other marks: 1 - main fault; 2 - reverse main; 3 - dip strike

- calculate the impedance, $E/H$, for the station affected by railway disturbances;

- attempt to separate non inductive regional telluric anomalies and signals;

- correlate the resistivity variations in time at the Villanova cave (VLN) with a seismic activity.

In our analysis we refer to seismic activity, restricting mainly to the periods of September 1987 and January/February 1988, when some stronger earthquakes have been recorded.

## 2. Instrumentation

The magnetic field at the two magnetotelluric stations was recorded with three-component torsion photoelectric magnetometers TPM (Jankowski et al., 1984).

For the measurements of the telluric field all three stations were equipped with telluric recorders and two electric lines, with length between 50 and 100 m, oriented N-S and E-W, where unpolarized electrodes have been used. The resistivity measurements were performed along two lines with the four electrode Wenner system installed in the Villanova cave, 65 m deep.

The digital data sampled each 20 s on a cassette tape were collected weekly and processed at IBM-PC computer with the use of various programs to analize them. Analog curves have been also reproduced for visual checking. Figs. 2 and 3 give examples of the magnetotelluric recordings.

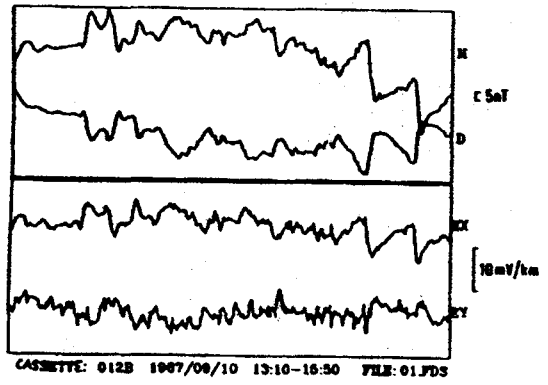


Fig. 2. Examples of recordings at the FDS station ($E_x$ = $E_{NS}$, $E_y$ = $E_{EW}$)

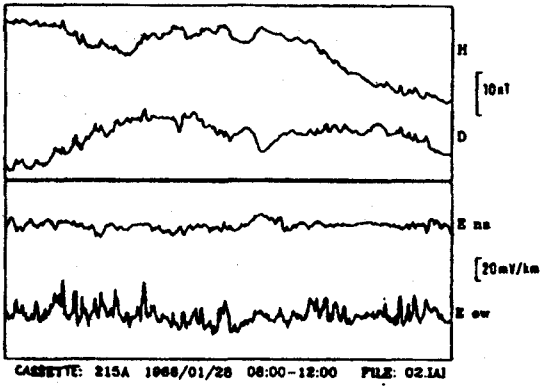


Fig. 3. Examples of recordings at the IAI station ($E_x$ = $E_{NS}$, $E_y$ = $E_{EW}$)

### 3. Electromagnetic induction

In a horizontally layered structure, magnetic components **H** and **D** induce telluric fields $E_{EW}$ and $E_{NS}$, respectively, but for a more complex structure the general relations between electric and magnetic components are, in time domain, as follows:

$$\begin{aligned} E_x &= Z_{11}(t) * H(t) + Z_{12}(t) * D(t) , \\ E_y &= Z_{21}(t) * H(t) + Z_{22}(t) * D(t) \end{aligned} \tag{1}$$

where * means convolution and $Z(t)$ are impulse responses ($E_{NS} = E_x$, $E_{EW} = E_y$).

The relations (1) in a frequency domain become:

$$\begin{vmatrix} \hat{E}_x(\omega) \\ \hat{E}_y(\omega) \end{vmatrix} = \begin{vmatrix} \hat{Z}_{11}(\omega) & \hat{Z}_{12}(\omega) \\ \hat{Z}_{21}(\omega) & \hat{Z}_{22}(\omega) \end{vmatrix} \begin{vmatrix} \hat{H}(\omega) \\ \hat{D}(\omega) \end{vmatrix}, \tag{2}$$

where $Z(\omega)$ is an impedance tensor and its components represent the respective transfer functions.

We have obtained both impedance and impulse response making calculations in time (Wieladek and Ernst, 1977) as also in frequency domain (Braitenberg and Zadro, 1990).

Impedance is analyzed with the method of complex singular decomposition (SVD) (LaTorraca et al., 1986) which leads to

$$Z(\omega)\ u_1 = \mu_1 v_1 ,$$

$$Z(\omega)\ u_2 = \mu_2 v_2$$

where $\mu_1$, $\mu_2$ are the singular complex values; the vectors $u_i$ (or $v_i$), $i = 1, 2$, are mutually orthogonal and correspond to two elliptically polarized states of $B(H, D)$ (or $T(E_x, E_y)$) -field with frequency $\omega$ and polarization direction $\alpha$ (or $\beta$).

Furthermore we define apparent resistivity and phase:

$$\rho_1 = 0.2\ P|\mu_1|^2, \qquad \varphi_1 = \text{phase}(\mu_1),$$

$$\rho_2 = 0.2\ P|\mu_2|^2, \qquad \varphi_2 = \text{phase}(\mu_2).$$

$P$ is the period in seconds, the B-field is measured in nT, the T-field in mV/km, and the resistivity in Ωm. Polarization angles are measured in degrees clockwise from north.

In Fig. 4 the result for the average impedance is graphed, where the averaging has been extended for selected intervals from September 1987 to February 1988. It is observed that the principal directions are almost aligned to the measuring axes. Furthermore the EW telluric component is observed to be affected by disturbances, for which reason we will restrict our further calculations to the NS telluric component at FDS station.

Each station is observed to have a typical polarization direction for both the magnetic and the electric fields. The distribution ellipse of the end-points of the field-vectors is calculated over a certain time interval. The direction of the major axis and the flattening of the ellipse give a measure of the polarization of the data.

In Fig. 4 the polarization directions for B- and T-field at FDS obtained for 12 subperiods each of 4 h length recorded during high magnetic activity in September, January and February are graphed. The mean orientations of the T-field can be summarized as follows:

| | FDS | IAI | VIL |
|---|---|---|---|
| for low frequencies: | | | |
| Dominant: | N40W-S40E | N80E-S80W | N70W-S70E |
| Secondary: | N80W-S80E | N40E-S40W | |
| for high frequencies: | | | |
| Dominant: | N70W-S70E | E-W | N70W-S70E |
| Secondary: | N50W-S50E | N-S | |

In an ideal 2-D model, the T-field should be polarized in a direction orthogonal to the structural lineaments. Moreover, the higher the electric field frequencies, the more the superficial layers should be involved. By considering the dominant responses, it results that, at

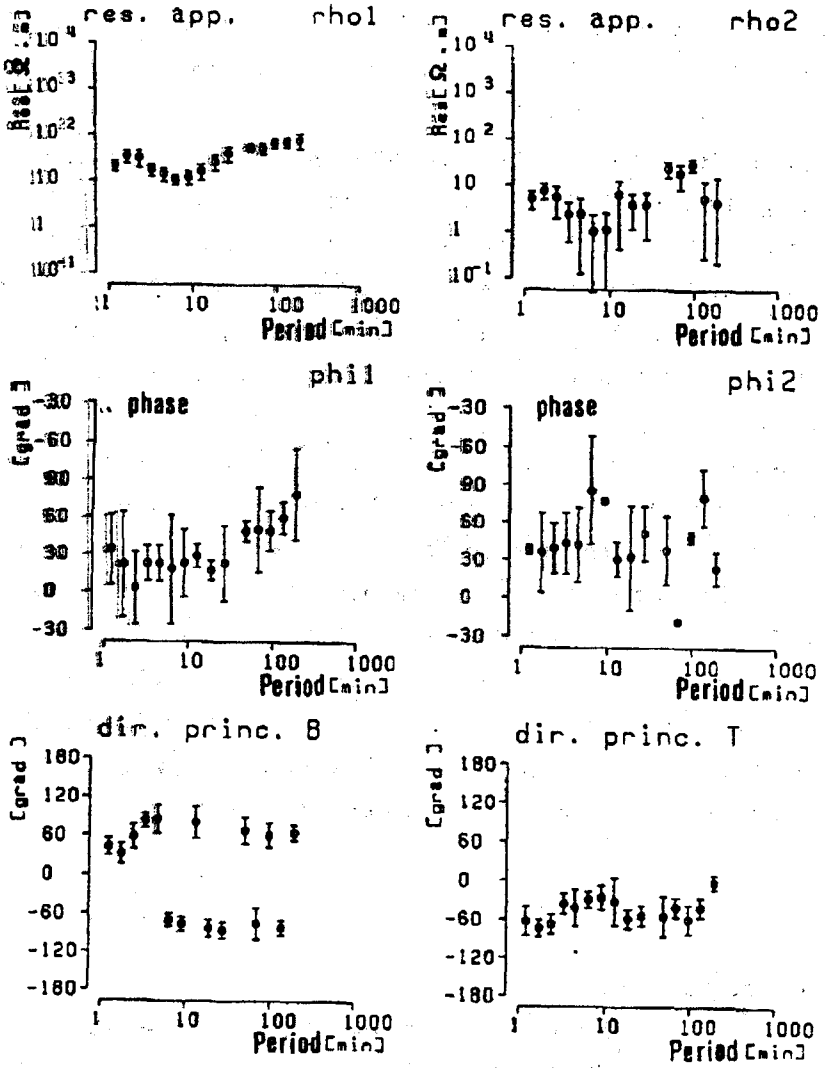


Fig. 4. Apparent resistivity, phase and principal direction at FDS

tens of km depth, the structures should be oriented as follows: N50E--S50W at FDS, N10W-S10E at IAI and N20E-S20W at VIL. At shallower depth, a counterclockwise rotation of 30° and a clockwise rotation of 10° is detected at FDS and IAI, respectively, whereas VIL maintains the same orientation. Of course, lateral inhomogeneities can greatly modify the 2-D assumption.

**4. Apparent resistivity changes**

Our aim was to find the possible changes of the apparent resistivity curves in time. Figure 5 gives different resistivity values (presented here for two periods). We have also plotted in the same figure the seismic events with $M \geq 2.6$. Analysing the data presented in this figure we can suppose that resistivity drops before some seismic events. Figure 6 presents different solutions for the apparent resistivity curves (here we put as an argument the period $T = 2\pi/\omega$ instead of the more commonly used $\sqrt{T}$), while Fig.7 presents this curves for the September and January data and the corresponding results of the inverse method (Wieladek and Nowożyński, 1989).

The lower diagram represents the integral conductance, from which we can find the resistivity structure at depth. The rough estimates of the resistivity values are as follows: 5-15 Ωm up to 15 km, and high resistivity values below. This fairly simplified structure shows a thick low-resistivity zone. Such a zone may correspond to a wide zone of the hypocentral planes dipping north (Amato et al., 1976; compare also Slejko et al., 1987). Apparently we can find some differences in the resistivity curves. The curve calculated for January 1988 exhibits lower resistivity values, also for long periods (i.e., for greater depth) with respect to the curves calculated for September.

However, taking into account the values of the mean errors, we shall not draw more implications from this observation.

One has to remember that not all the data, and consequently not all the results, are contaminated with the same errors. On account of high magnetic activity, we are able to concentrate on the September and January data. Such a choice has also this advantage that it corresponds to a rather more remarkable seismic activity.

Knowing the transfer function (or impulse response) between magnetic and telluric fields we can apply the following procedure. The magnetic data recorded permit us to calculate the expected (predicted) telluric field by formula (1). Figures 8 and 9 show the original telluric signal at the FDS station, beneath which we have plotted the calculated (predicted) telluric curve and further down we have given the

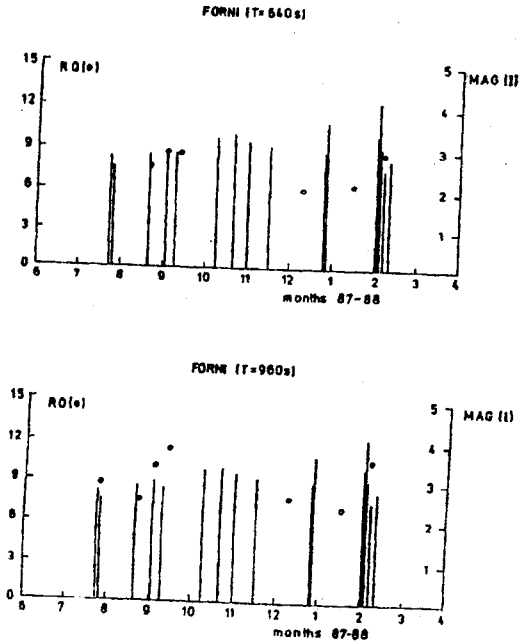


Fig. 5. The apparent resistivity values (for two periods) and the earthquake magnitudes ($M \geq 2.6$)

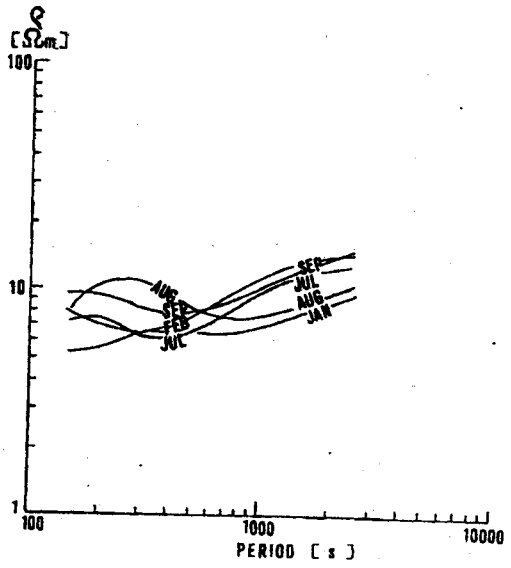


Fig. 6. The curves of apparent resistivity at station Forni di Sotto calculated for different months during the days with high magnetic activity

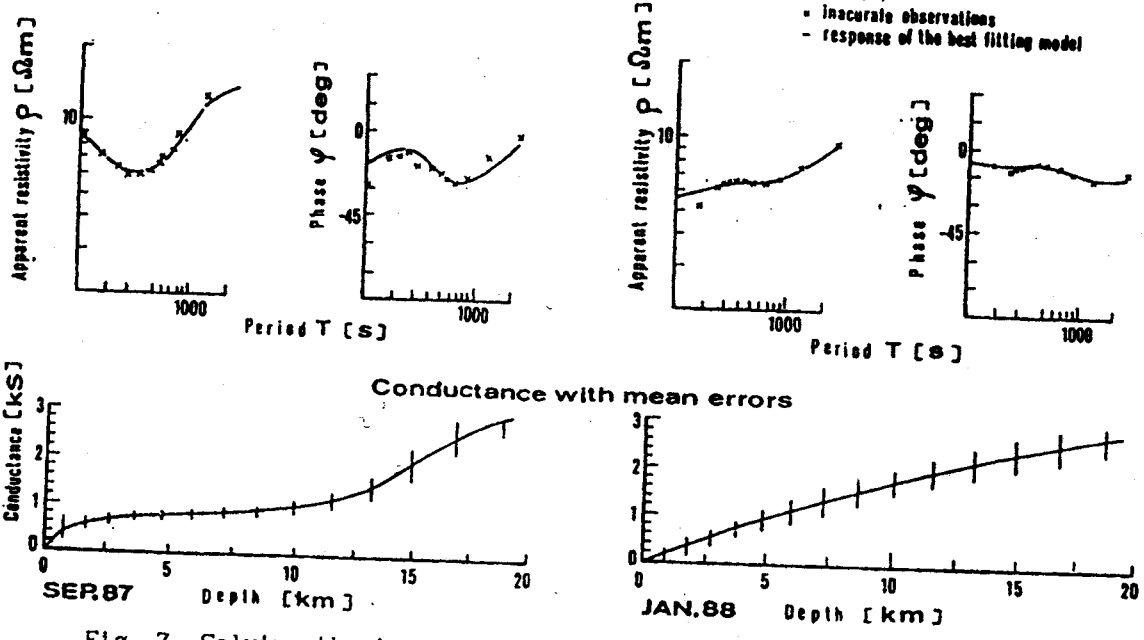


Fig. 7. Solving the inverse problem: lower diagrams give the integral conductance for September and January data

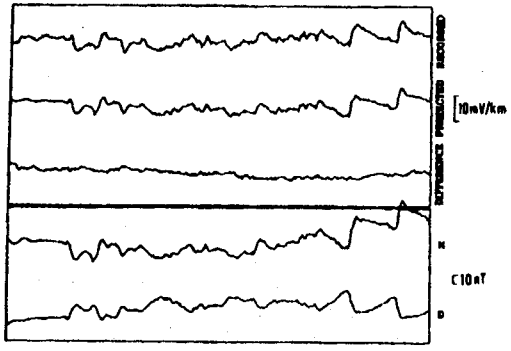


Fig. 8. Examples of original and predicted recordings at the FDS station (Forni, September - event 1)

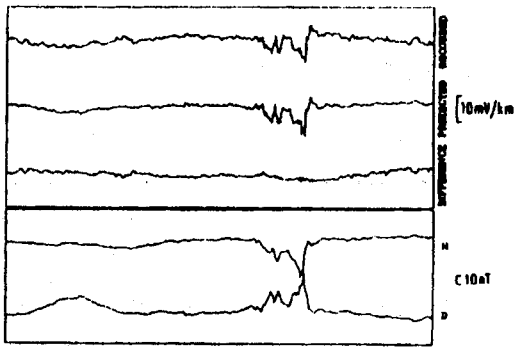


Fig. 9. Examples of original and predicted recordings at the FDS station (Forni, January - event 2)

respective difference. In this procedure we have used the average impulse response calculated for several stronger magnetic events in September 1987 and January 1988. The good agreement between predicted and observed telluric field can be seen in Figs 8 and 9.

## 5. Artificial disturbances of electromagnetic field

The recordings, both magnetic and telluric, at the IAI station frequently exhibit considerable artificial variations due to the electric trains. Fortunately a rough examination of these disturbances indicates a nearly constant ratio of magnetic to electric components. First we can eliminate the natural magnetic variations subtracting from the magnetic field in IAI the corresponding component recorded in FDS (this station is not much disturbed by the artificial sources):

$$H' = H^{IAI} - H^{FDS} . \qquad (3)$$

Figure 10 presents the artificial disturbances of magnetic and electric fields.

With $H'$ we can try to calculate the impulse response (1) for the artificial variations only. But the calculations have proved that it suffices to take simply one constant factor as the impulse response

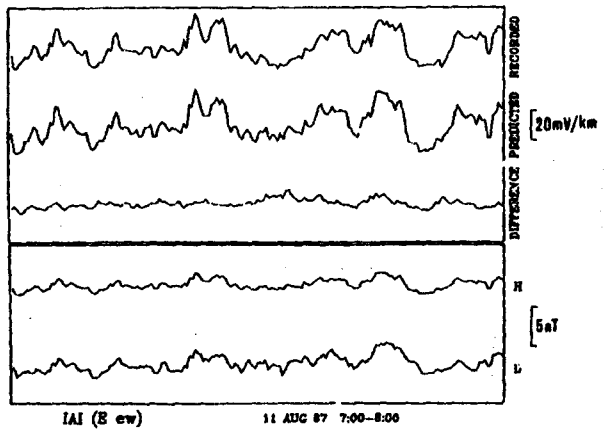


Fig. 10. The railway disturbances at the IAI station; examples of original and predicted recordings

between disturbances of $E_y^{IAI}$ (denoted as E) and H':

$$E(t) = I\ H'(t), \tag{4}$$

where the coefficient $I$ can be called an impedance disturbance factor. In each half hour for several events we can trace its possible changes in time, as $I$ depends also in some way on the actual resistivity structure at depth. Figure 11 presents the time variations of the impedance disturbance factor for several events. We have taken into account only the results with small mean square errors.

Assuming that $I$ is constant we can eliminate the artificial disturbances from the EW component of the telluric field in the IAI station:

$$E'(t) = E(t) - I\ H'(t). \tag{5}$$

The lower part of Fig. 10 shows that the method applied brings reasonable results and good fitting of recorded and calculated curves. In Fig. 10 this function is marked as the difference between the recorded and calculated events.

A more sophisticated method should rely on the appropriate correlation procedure which also includes the elimination of the natural magnetic variations and the artificial disturbances. In fact $E'(t)$ is expected, by virtue of formula (5), to represent the time variation of the telluric field at IAI. Thus it could be adequate for comparison with the corresponding telluric records in FDS. The $E_y$ component at FDS

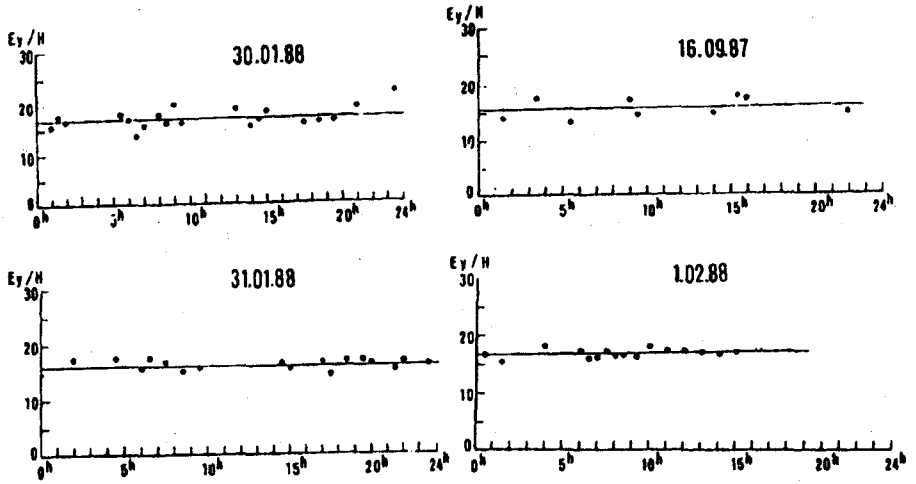


Fig. 11. Examples of day recordings of the impedance factor at the IAI station

is almost unaffected by magnetic variations. However, more close insight into the proposed procedure reveals that also small local magnetic variations at FDS may be transferred by equation (3) and then (5) into the function $\mathbf{E}'(t)$. Hence, we cannot be sure whether a correlation between $E_y$ at FDS and $\mathbf{E}'$ indicates a correlation between the telluric fields at FDS and IAI or whether it shows a correlation between the telluric field in FDS and the local magnetic variations also in FDS. Such an alternative is to be underlined.

## 8. Common signals

To eliminate natural variations of magnetic induction in the FDS station and railway disturbances in the IAI station we tried to find the common field signals. The magnetic induction effects at the IAI station are much smaller and can be neglected. The common part is an average curve from the two stations multiplied by the correlation coefficient calculated for each half-hour interval (moving window):

$$\text{Common} = \frac{E^{IAI} + E^{FDS}}{2} R. \qquad (6)$$

As $E^{IAI}$ and $E^{FDS}$ we have used the E' field and the EW ($E_y$) component at FDS.

The common field signals, due to the procedure applied, are almost free of the artificial disturbances. However, some disturbances of the magnetic field in FDS could remain in the common signals. High common values may therefore indicate the existence of some others electric sources. For small values of correlation coefficient $R$ the common curve becomes flat.

Figure 12 gives an example of calculated common signals for September, while Fig. 14 gives the examples for January/February before a series of earthquakes.

In Figs. 13 and 15 we present the values of variances of the common signals (taken for six hour intervals).

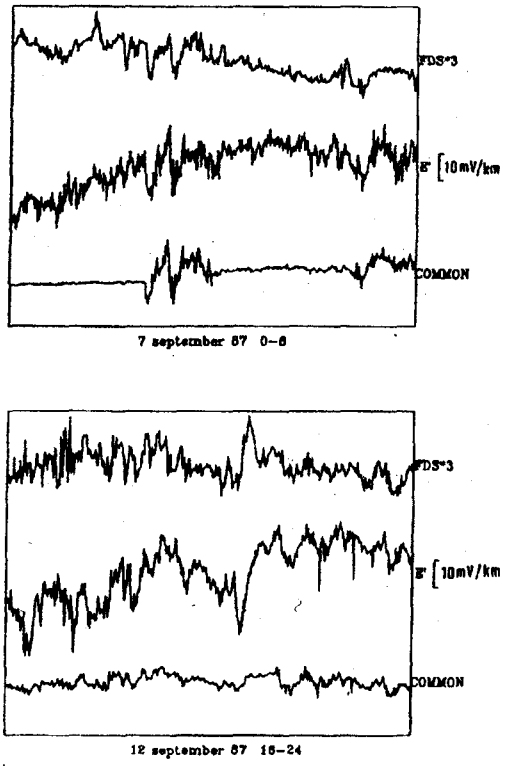


Fig. 12. The EW component of telluric field at station FDS and E' at IAI; the lower curve presents the common part (explanation in the text) - the September data

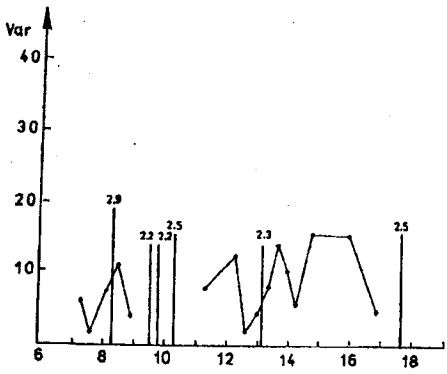


Fig. 13. Time changes of the variances of the common signals and the seismic activity in September (events with magnitude bigger than 2.2)

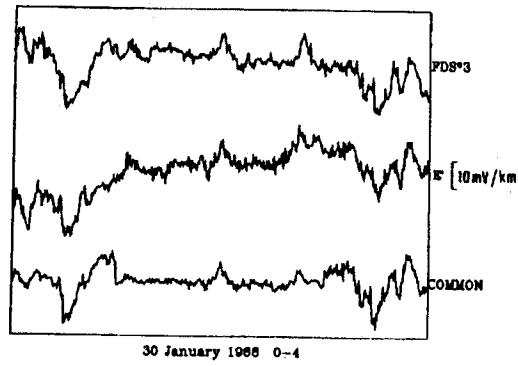


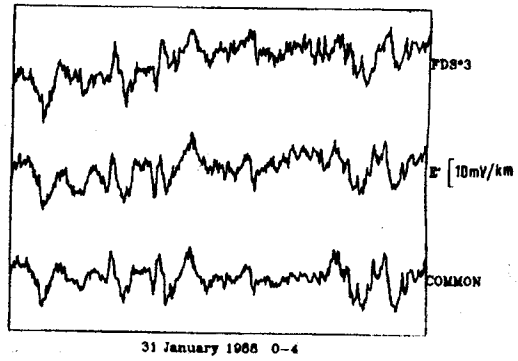


Fig. 14. The EW component of telluric field at station FDS and E' at IAI; the lower curve presents the common part (explanation in the text) - the January/February data

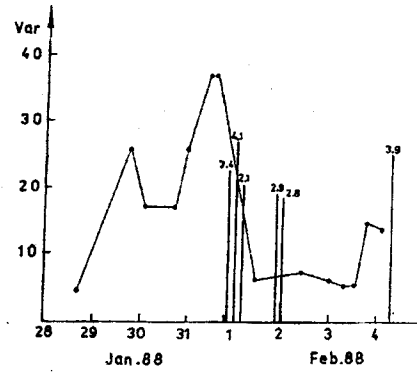


Fig. 15. Time changes of the variances of the common signals and the seismic activity at the end of January and the beginning of February 1988 (events with magnitude bigger than 2.0)

The earthquake events are marked with the corresponding magnitudes. The changes of variances in time before the earthquakes in the beginning of February 1988 can suggest a possibility of existence of premonitory effects.

## 7. Electromagnetic energy flux

Now we will present another method applied for an analysis of the recorded magneto-telluric fields.

To see if any electromagnetic field can be generated in the Earth interior the calculation of the Poynting vector is applied. The Poynting vector S is defined as a vector product of electric field E and magnetic field H:

$$\mathbf{S} = \mathbf{E} \times \mathbf{H}.$$

The value of Poynting vector is interpreted as a flux of energy flowing through a surface perpendicular to this vector. Let the Earth's surface be identified with $z = 0$ (the $z$-axis is directed downward). A very simple, one-dimensional model of resistivity will be considered.

Let us suppose that the magneto-telluric field at the Earth's surface can be treated as a superposition of the incident and reflected electromagnetic plane waves and also of the fields related to the non-inductive signals such as SES. In the absence of non-inductive signals, an average flux of the energy transferred through the Earth surface should always show a positive difference between the electromagnetic energy flux $S_{IN}$ transferred into the Earth and the flux $S_{REF}$ transferred out of the Earth.

Let us define the reflexion coefficient as a ratio of the flux of the reflected wave to that of the incident wave:

$$R = \frac{S_{REF}}{S_{IN}} \tag{7}$$

and the transmission coefficient as a

$$T = 1 - R. \tag{8}$$

In the absence of non-inductive signals, there should always be $0 \leq T \leq 1$. The case $T < 0$ may indicate an electromagnetic source inside the Earth.

Hereafter we propose the method to calculate the transmission coefficient. First we have divided the electromagnetic field into incident and reflected plane waves (internal and external part). Let us consider one polarization only and $E_x(z,t)$, $E_y(z,t)$ to be observed

(horizontal $E_{NS}$ and $D$ components of the electromagnetic field) on the Earth's surface. If $E_x^{IN}$, $B_y^{IN}$ and $E_x^{REF}$, $B_y^{REF}$ are the electromagnetic fields of incident and reflected waves, we have Maxwell's equation solution:

$$E_x = E_x^{IN}(t - \frac{z}{c}) + E_x^{REF}(t + \frac{z}{c}),$$
$$B_y = B_y^{IN}(t - \frac{z}{c}) + B_y^{REF}(t + \frac{z}{c}) \tag{9}$$

where:

$$E_x^{IN} = cB_y^{IN}, \qquad E_x^{REF} = -cB_y^{REF}.$$

It is easy to see that:

$$E_x^{IN} = \frac{1}{2}(E_x + cB_y), \qquad E_x^{REF} = \frac{1}{2}(E_x - cB_y). \tag{10}$$

Similarly for the observed orthogonal fields $E_y(z,t)$, $B_y(z,t)$ ($E_{EW}$, H) we get the expression:

$$E_y^{IN} = \frac{1}{2}(E_y - cB_x), \qquad E_y^{REF} = \frac{1}{2}(E_y - cB_x). \tag{11}$$

After the field division, incident $E_x^{IN^2}$, $E_y^{IN^2}$ and reflected $E_x^{REF^2}$, $E_y^{REF^2}$ power spectra have been calculated by the maximum entropy method (Wieladek et al., 1975) have been calculated. The respective incident and reflected spectra for orthogonal polarization have been summed, giving the total incident and reflected power spectra proportional to $S_{IN}$ and $S_{REF}$.

Transmission coefficient (8) has been then calculated. For an analysis, the data from Forni di Sotto (FDS) station were used. The data are presented as 3-D plots (Fig. 16) and 2-D maps (Fig. 17), as a function of the date of observation and $\sqrt{\text{period}}$. In Fig. 17 one can see maps in which contours for negative transmission coefficient values are only marked. Figures 16 and 17 present results for September 1987 data, while Figs. 18 and 19 show results for January/February 1988. The day number and time is plotted in decimal format on horizontal axes and $10^{-1}\sqrt{\text{period}}$ is marked on vertical axes. The seismic events for the Friuli region with magnitude greater then 2.0 for September and greater then 2.0 for January/February are marked on the plots. One can see very

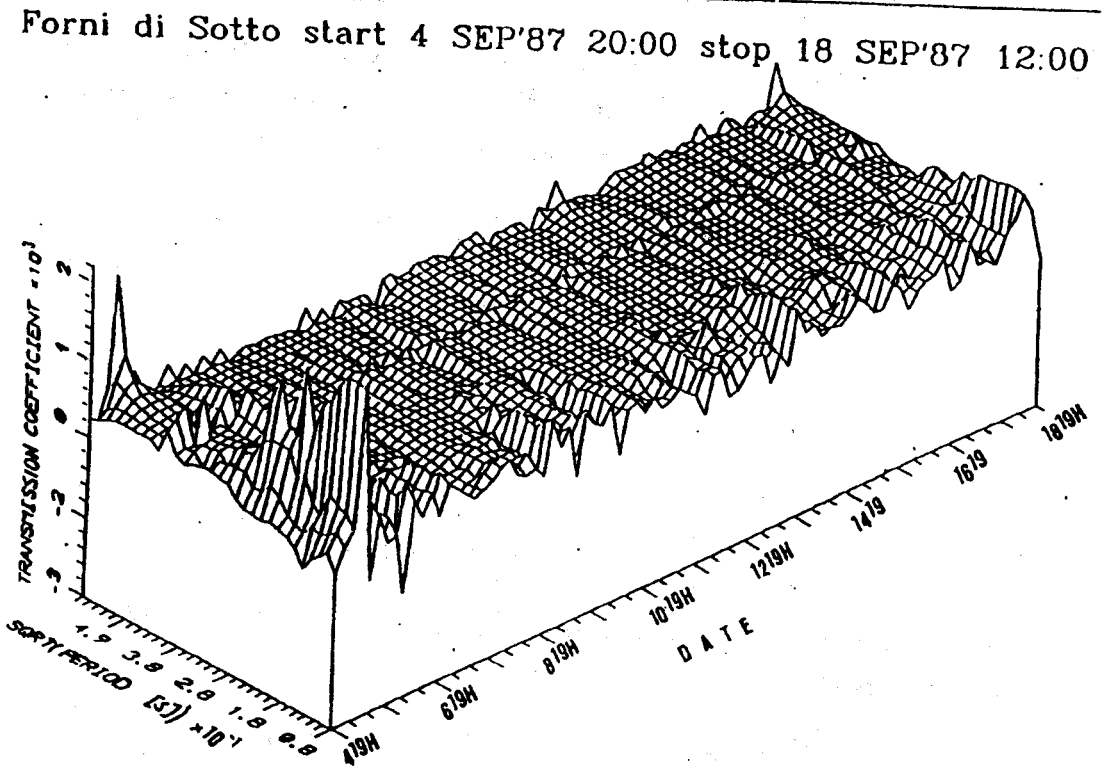


Fig. 16. The map ($x$ - date, $y$ - $\sqrt{T}$) of the transmission coefficients (negative values) in September

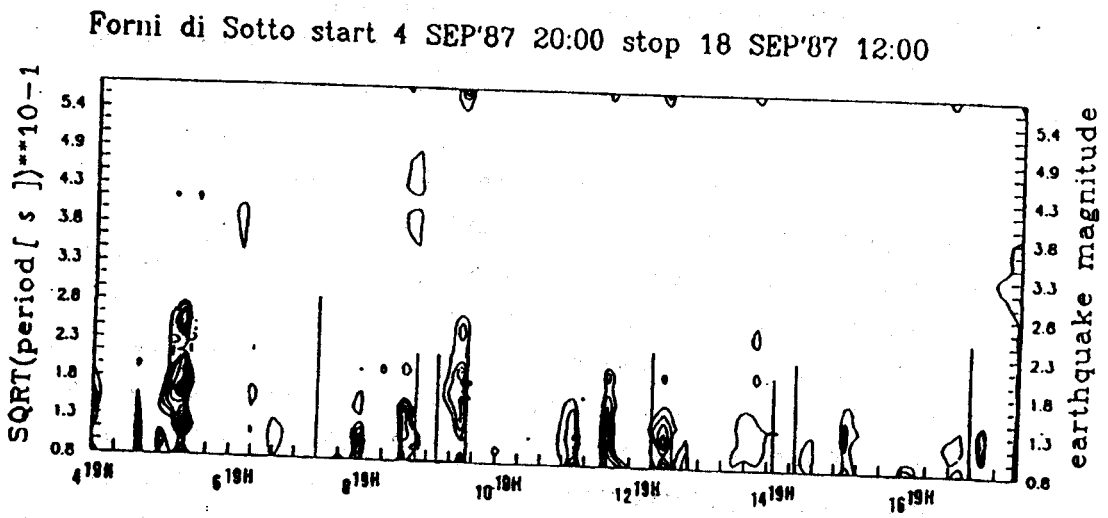


Fig. 17. The negative isolines ($x$ - date, $y$ - $\sqrt{T}$) of the transmission coefficients in September; seismic events with magnitude bigger than 2.0

few moments when the transmission coefficient $T < 0$; it seems that these moments precede earthquake events, at least the stronger ones - see the case of January/February, when a series of relatively strong earthquakes have occurred after very low seismic activity in January, which may have caused the big energy deposit to break down.

A more sophisticated procedure can be applied in order to increase the signal-to-noise-ratio.

For example we can substract the predicted electric field from the observed one and calculate a part of the Poynting vector related only to this difference:

$$S = (E_{obs} - E_{pred}) \times H . \qquad (12)$$

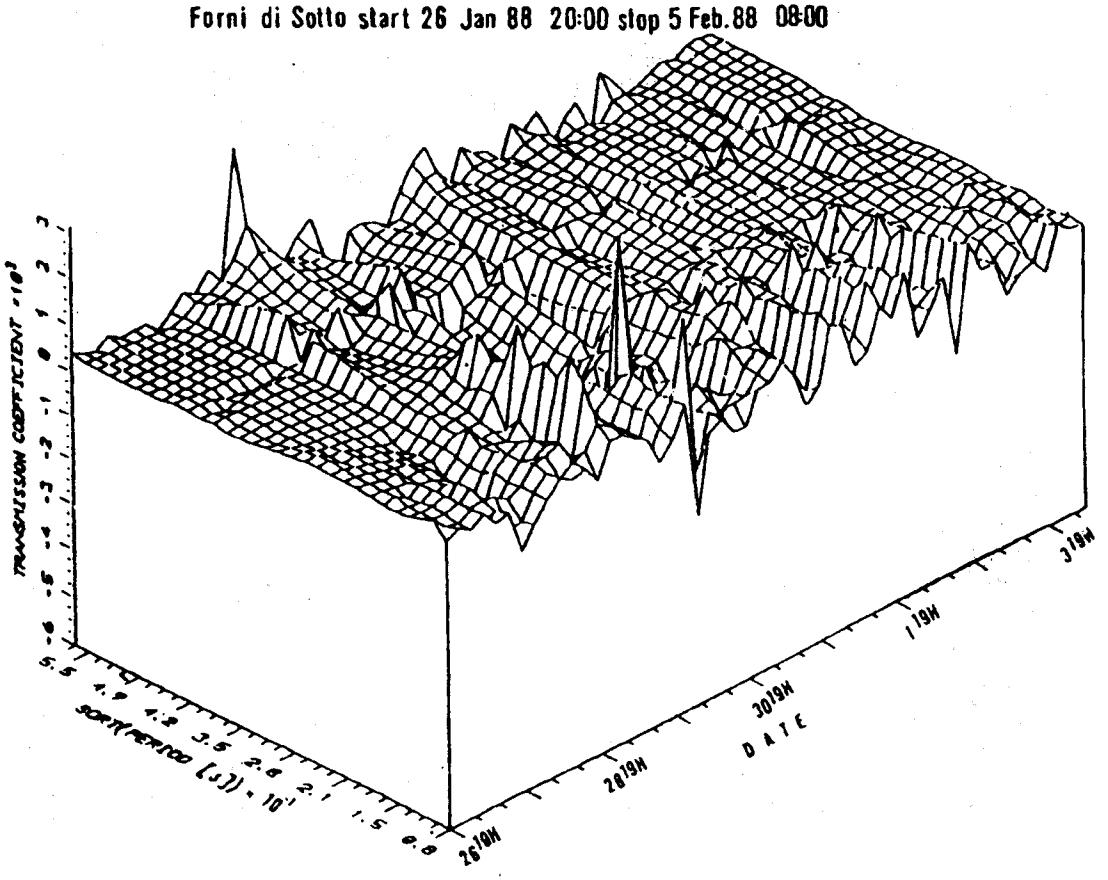


Fig. 18. The map ($x$ - date, $y$ - $\sqrt{T}$) of the transmission coefficients (negative values) in January/February

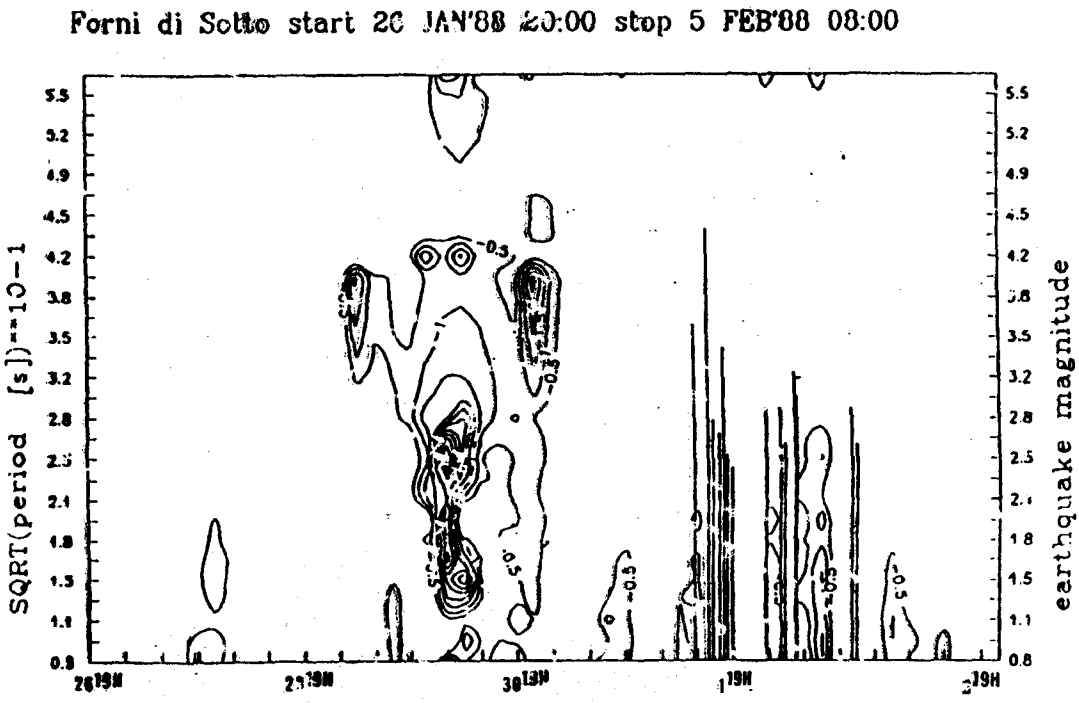


Fig. 19. The negative isolines ($x$ - date, $y$ - $\sqrt{T}$) of the transmission coefficients in January/February; seismic events with magnitude bigger than 2.0 are marked along the axis

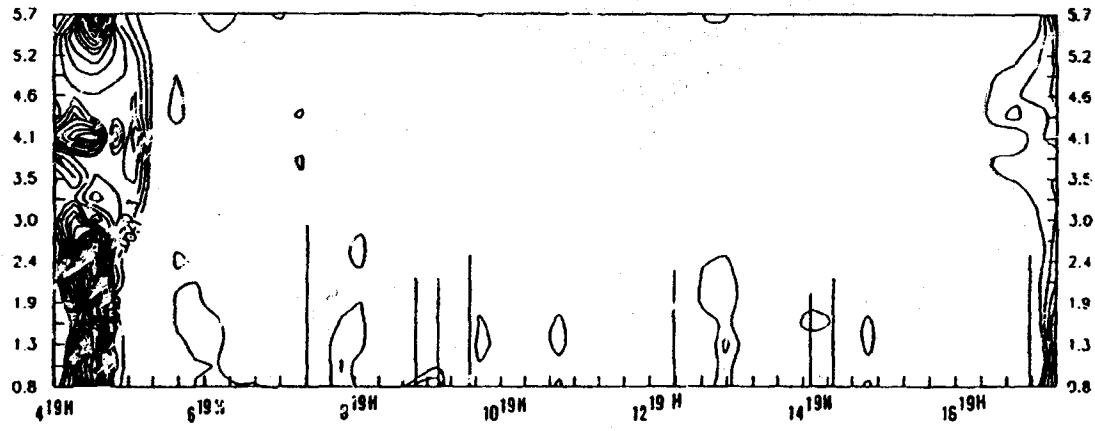


Fig. 20. The negative isolines ($x$ - date, $y$ - $\sqrt{T}$) of the transmission coefficients modified according to formula (12) in September; seismic events with magnitude bigger than 2.0

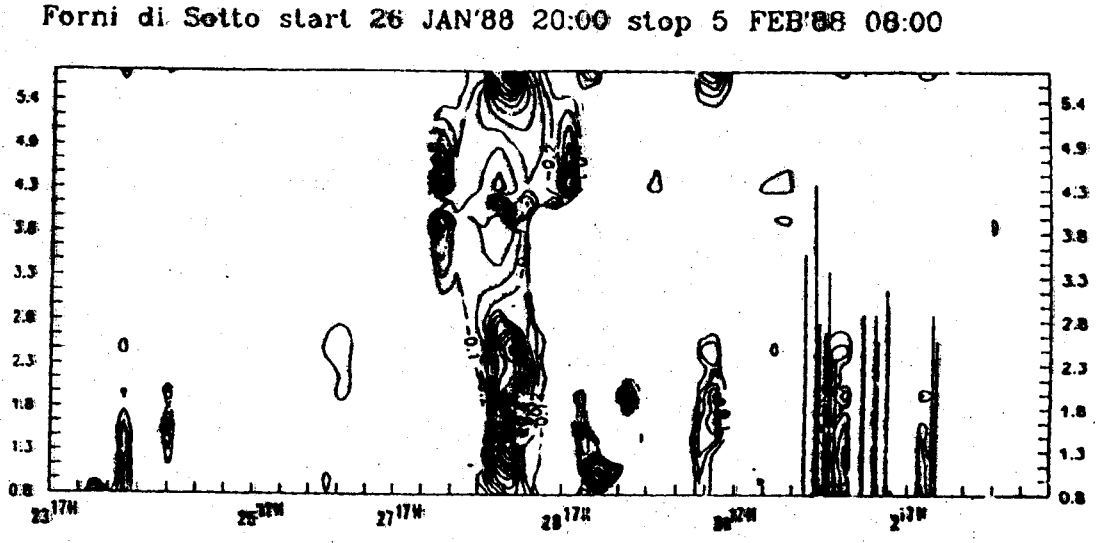


Fig. 21. The negative isolines ($x$ - date, $y$ - $\sqrt{T}$) of the transmission coefficients modified according to formula (12) in January/February; the seismic events with magnitude bigger than 2.0 are marked along the axis

We should be aware, however, that procedures of such type highly increase the values of errors. Figures 20 and 21 give the negative values for the transmission coefficient calculated according to equation (12) for September and January data, respectively.

## 8. Measurements of resistivity variations

From January 1988 to June 1989 we recorded the resistivity variations at station VIL, two measurement lines of the Wenner method, situated almost perpendicularly to each other ($X$, $Y$), were installed in a deep cave. The digital recording device recorded the relative resistivity values every 20 s.

The recordings are presented in Figs 22 and 23 ($X$ = NS and $Y$ = EW components); some very big resistivity changes are related to atmospheric precipitations, also the daily variations can be observed on both components.

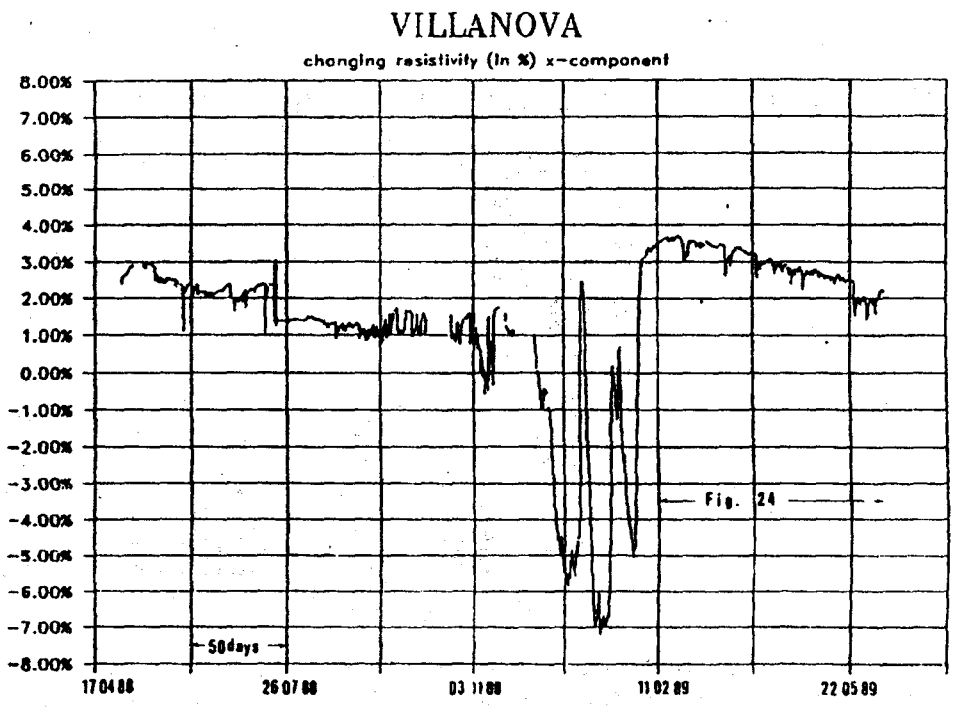


Fig. 22. The resistivity variations at VIL station - *x*-component

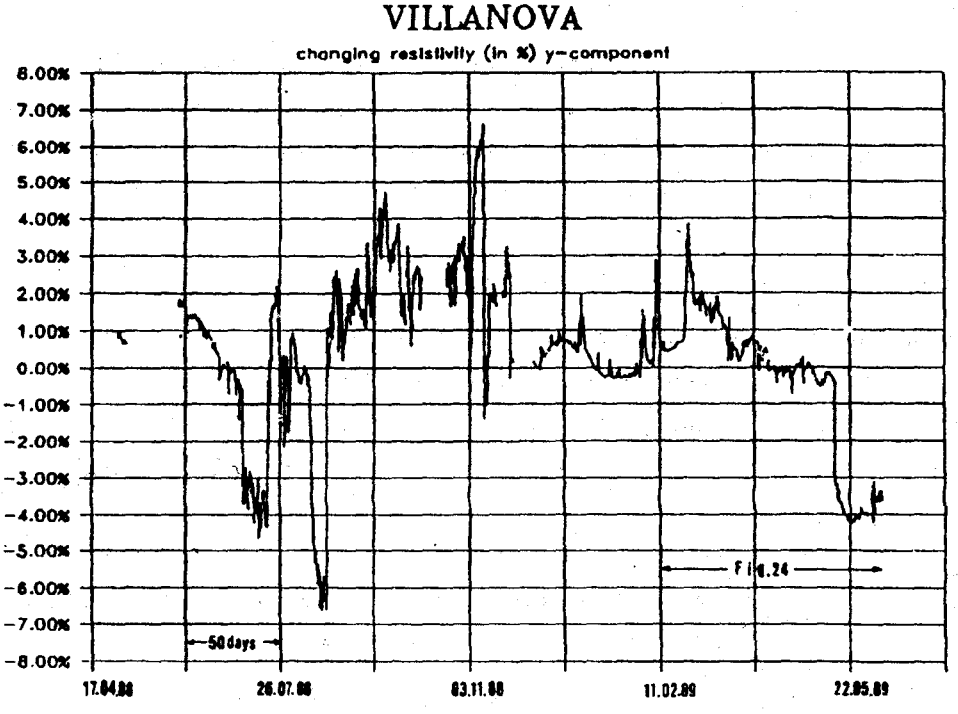


Fig. 23. The resistivity variations - *y*-component

At last, in Fig. 24 the *X* and *Y* recording are presented, and some earthquake events are marked by arrows; a drastic drop of resistivity may be related to the earthquake of 13 May 1989 (21:55).

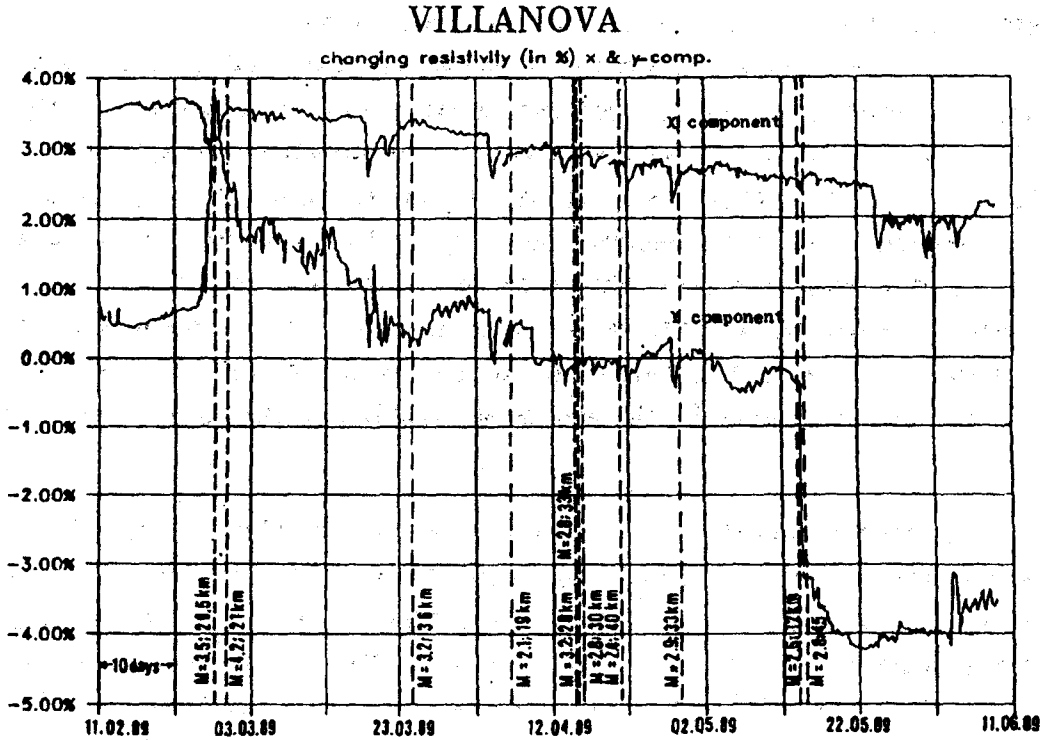


Fig. 24. The resistivity variations and possible correlation with some seismic events shown by arrows

## 9. Discussion on current generation at a seismic source

There are some attempts to explain the current generation before an earthquake that could take place in a source preparation zone. One of the approaches is related to polarization/depolarization currents (e.g. Varotsos and Alexopoulos, 1984, assume polarization processes under the influence of stresses). Another approach is related to motion of charge dislocations (Gokhberg et al., 1985; Teisseyre, 1989; Slifkin, 1990).

In the charge dislocation model (Teisseyre, 1989) an earthquake zone is represented arranged defects (dislocation arrays, cracks), arranged in parallel, while an earthquake preparation and energy release

processes are determined by a propagation of these defects and the changes in their density. The results of the Rebound Theory (Teisseyre, 1985; 1988) are used here in order to get a model of crack development and fracturing processes in time along a fault plane.

All considerations are based on the assumption that a moving element, representing the extended earthquake source zone, generates the electric current, the intensity of which is proportional to the velocity of defect propagation and to defect density (the same assumptions can be found in other papers, see, e.g., Gokhberg et al., 1985; as a result of charge relaxation and of charge excitations in the process of dislocation motion and interaction with ionic vacancies we can treat a charge of a moving dislocation as bounded to a dislocation core). The current density vector in the source is parallel to the velocity vector:

$$j = N V$$

We assume also that the concentration of oriented moving defects may induce resistivity anisotropy which depends on the state of the earthquake preparation process (K. Teisseyre, 1989). Some remarkably big changes in electric field can be found according to the theory outlined above (K. Teisseyre, 1989). There are typical bay-type anomalies and also more sharp signals (like the SES), having usually the same orientation as the bay anomalies. The sharp signals are related both to the induced resistivity anisotropy and to the high increase of dislocation density before an earthquake event.

Recent discussions on this problem by Teisseyre and Utada (1991), indicate a possibility of combining these two approaches into a model of polarization process stimulated by a motion of dislocations. Such a process is associated with the transition from isotropic to stress induced anisotropic properties in an extended earthquake source zone; here, a dilatancy phase plays a special role.

The polarization effects relate to point defects and exhibit a certain relaxation time (we are not considering the instantaneous polarization which disappears immediately after the electric field is removed). The relaxation time depends on dipole rotations under a given temperature and pressure condition:

$$\tau = \tau_0 \exp(\frac{g^m}{kT}),$$

where $g^m$ is the Gibbs migration energy (for point defects) which depends on stresses (pressure). Depending on sign of the derivative $\partial g^m/\partial p$, the relaxation time can decrease or increase with pressure, while it always decreases with temperature. If the migration volume $v^m = \partial g^m/\partial p$ is positive, the value of $\tau$ increases with $p$. In the case of dilatancy we have $\delta p < 0$ ($\delta v > 0$), hence the relaxation time would decrease.

We shall notice here that the piezoelectric effect is related to motion of charge dislocations, while the polarization effect is related to rotations of dipoles and thus concerns point defects. Here the piezoelectric properties, usually related to some anisotropic crystal structures, may be combined with the induced anisotropy caused by the fracturing related structures and these properties appear in the dilatancy phase.

Dilatancy causes a certain decrease of internal pressure; the material in a source zone undergoes expansion $dv > 0$. Parallel with this process, the dislocations and cracks develop and group already in one preferable direction (related to the future direction of fracturing).

Thus we assume that the premonitory processes cause the dipole rotations (polarization) partly due to electric field of the charge bearing dislocations and partly due to a kind of forced rotation: reorientation of some material elements along slip or microfracturing planes. These processes can take place in an extended earthquake source zone.

Mathematically this is expressed by polarization dependence on the rate of dislocation density increase (causing crack development and branching); at the moment of dilatancy the crack density rapidly increases. When dislocations start to group in the dislocation arrays we can expect non-reversible processes of crack formation, or we can say the formation of microfracturings. Due to interaction between dislocations (similarly we have crack interaction) a transition from the isotropic state to a phase of oriented properties will occur in a rather short time interval, especially when one takes into account high dislocation density.

A dislocation in crystal structure is formed by an excess or removal of a half-plane of atoms. At the edge of this half-plane a dislocation line is thus formed, around which physical fields related to it are concentrated. This is a singular line. In ionic structure we will thus have an excess or a removal of a line row of ions along the dislocation line; in this case the dislocation is a charged one (Whitworth, 1975).

When a dislocation moves, it affects the concentration and orientation of point defects in the extended source zone. The dipoles are formed by point defects that could migrate around an atom - this is called a bound defect motion in reorientating dipoles. Thus, an influence of charged dislocations on point defects is expressed by polarization of dipoles through a bound defect migration (reorientation of dipoles).

A transient polarization current will be thus related to the influence of linear defects (dislocation arrays and cracks) on point vacancies. Such a polarization current will highly magnify the electric field of charge dislocations.

The density rate of vacancies (and thus also dipoles) which undergo migration (causing dipole rotation) would be thus proportional to the density rate of dislocations, which affects these point defects.

Electrical polarization $P$ is proportional to density of dipoles and we assume, as proposed above, that the density rate of dipoles $dn/dt$ is proportional to the density rate of dislocations $dN/dt$ acting on ionic vacancies.

We get for the current density:

$$j = \frac{dP}{dt} = p\,\frac{dn}{dt} \propto \frac{dN}{dt} \tag{13}$$

where $p$ is an average dipole moment.

In the Earthquake Premonitory and Rebound Theory (Teisseyre, 1985, 1987, 1991) the definite relations combine dislocation density, stresses and bulk (mean) dislocation velocity $V$. In a simple case of motion in the $x$-direction and taking only a shear stress field S we have the following relation

$$N = \frac{1}{2\mu}\frac{dS}{dx} . \tag{14}$$

Combining the above formulae we come to the relation:

$$j \propto \frac{dS}{dx} = \frac{1}{V}\frac{d^2S}{dt^2} . \tag{15}$$

A current density is thus proportional to the second time derivative of stresses (assuming that the changes of the velocity field can be neglected).

From numerical solutions we can take after Teisseyre (1985) an example of stress increase and then determine its derivatives (Fig. 25). Thus the maximum of the current intensity generated at the source evidently precedes the seismic event. The time lag depends, however, on material properties and on stress concentration rate in a focal zone.

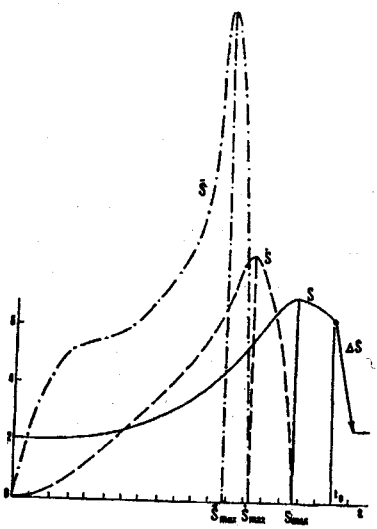


Fig. 25. An example of stress accumulation before a seismic event with its first and second derivatives; the electric current generated in a source zone is proportional to the second time derivative of stresses

## 10. Conclusions

During the time period from July 1987 to June 1988 the observations in the Friuli seismic zone have taken place, including two magne-

totelluric stations and one telluric and resistivity station. In the region the presence of industrial noise and railway disturbances cannot be completely excluded.

Under these circumstances, identification of observed sharp telluric signals as SES, is not possible. Nevertheless, some interesting signals were recorded (Fig. 26). Therefore, our studies were directed to include the magnetic recordings and to verify whether some increase in the telluric activity, not correlated with magnetic field, may be related to forthcoming earthquakes. The application of the presented methods of common field calculations and of the energy flux transmission gave some results which brought indications of increase of telluric activity before earthquakes.

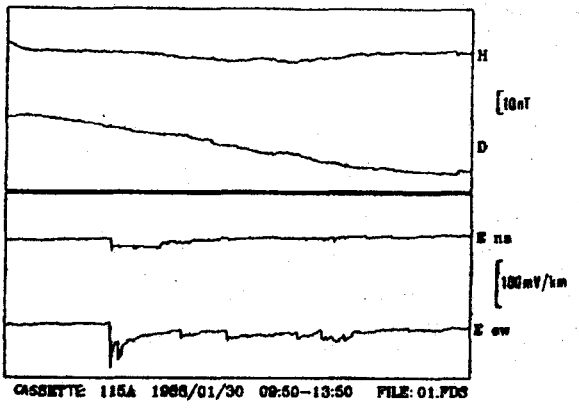


Fig. 26. Some interesting signals before earthquake series in February 1988

Continuous measurements of resistivity at VIL station showed some variations which can be correlated with forthcoming earthquakes.

## References

Amato A., Barnaba P.F., Finetti I., Groppi G., Martines B., and Muzzin A., 1976, *Geodynamic outline and seismicity of Friuli Venetia Julia region*, Boll. Geofis. Teor. Appl., 19, 217-256.

Braitenberg C., and Zadro M., 1990, *The magnetotelluric campain in Eastern Alps, NE-Italy: Regional and local 2-D responses of the seismic zone*, Boll. Geofis. Teor. Appl., 32, 141-156.

Gokhberg M.B., Gufeld I.L., Gershenzon N.I., and Pilipenko V.A., 1985, *Electromagnetic effects during rupture of the Earth's crust*, Izv. Akad. Nauk SSSR, Fiz. Zemli, 21, 1, 52-63.

Jankowski J., Marianiuk J., Ruta A., Sucksdorff C., and Kivinen M., 1984, *Long term stability of a torque-balance variometer with photoelectric converters in observatory practice*, Geophys. Surv., 6, 367-380.

LaTorraca M., Madden T.R., and Korringa J., 1986, *An analysis of the magnetotelluric impedance for three dimensional conductivity structures*, Geophysics, 51, 1819-1829.

Rikitake T., 1976, *Earthquake Prediction*, Elsevier Sci. Publ. Comp., Amsterdam.

Slejko D., Carulli G. B., Carraro F., Castaldini D., Cavallin A., Doglioni C., Iliceto V., Nicolich R., Rebez A., Semenza E., Zanferreri A., and Zanolla C., 1987, *Modello sismotettonico dell'Italia Nord - Orientale*, C.N.R. Gruppo, Nazionale per la Difesa dai Terremoti, Trieste.

Slifkin L., 1990, *Dislocation Model*, present. at Intern. Conf. Measurements and Theoretical Models of the Earth's Electric Field Variations Related to Earthquakes, 6-8 February 1990, Athens.

Sobolev G.A., 1975, *Application of electric method to the tentative short-term forecast of Kamchatka earthquake*, Pure Appl. Geophys., 113, 229-235.

Stopiński W., and Teisseyre R., 1982, *Precursory rock resistivity variations related to mining tremors*, Acta Geophys. Pol., 30, 293-320.

Teisseyre K., 1989, *Anisotropy of electric resistivity related to crack processes before fracturing*, Acta Geophys. Pol., 37, 185-192.

Teisseyre R., 1985, *New earthquake rebound theory*, Phys. Earth Planet. Inter., 39, 1-4.

Teisseyre R., 1988, *Earthquake rebound theory: in-plane motion with crack branching*, Acta Geophys. Pol., 36, 301-307.

Teisseyre R., 1991, *Electrotelluric anomalies generated by the moving dislocations*, present. at Intern. Conf.: Measurements and Theoretical Models of the Earth's Electric Field Variations Related to Earthquakes, 6-8 February 1990, Athens.

Teisseyre R., and Utada H., 1991, *Piezo stimulated dilatancy current (PSDC) before earthquakes* (in preparation).

Varotsos P., and Alexopoulos A., 1984, *Properties of the variations of the electric field of the earth preceding earthquakes. II - Determination of epicenter and magnitude*, Tectonophysics, **110**, 99-125.

Wieladek R., Bromek A., and Ostrowski J., 1975, *Modefied maximum entropy method of determining power spectra of stationary processes with a program in Fortran*, Publ. Inst. Geophys. Pol. Acad. Sci., **96**, 3-32.

Wieladek, R., and Ernst, T., 1977, *Application of the method of least squares to determining impulse responses and transfer functions*, Publ. Inst. Geophys. Pol. Acad. Sci., G-1 (110), 3-12.

Wieladek R., and Nowożynski K., 1989, *The accuracy of solution of one-dimensional magnetotelluric inverse problem*, Acta Geophys. Pol., **37**, 37-70.

Withworth R., 1975, *Charged dislocations in ionic crystals*, Adv. Phys., **24**, 203-304.

Yamazaki Y., 1975, *Precursory and coseismic resistivity changes*, Pure Appl. Geophys., **113**, 219-229.

Manuscript received 20 December 1990